Ocean Sci. Discuss., 10, 2157–2206, 2013
www.ocean-sci-discuss.net/10/2157/2013/
doi:10.5194/osd-10-2157-2013

Ocean Science
Discussions
Open Access

Evaluation of MERIS products from Baltic Sea coastal waters rich in CDOM

J. M. Beltrán-Abaunza[1], **S. Kratzer**[1], **and C. Brockmann**[2]

[1]Department of Ecology, Environment and Plant Sciences, Stockholm University 106 91, Stockholm, Sweden
[2]Brockmann Consult GmbH, Max-Planck-Str. 2, 21502 Geesthacht, Germany

Received: 26 September 2013 – Accepted: 4 November 2013 – Published: 28 November 2013

Correspondence to: J. M. Beltrán-Abaunza (jose.beltran@su.se)

Published by Copernicus Publications on behalf of the European Geosciences Union.

Abstract

In this study, retrievals of the medium resolution imaging spectrometer (MERIS) reflectances and water quality products using 4 different coastal processing algorithms freely available are assessed by comparison against sea-truthing data. The study is based on a pair-wise comparison using processor-dependent quality flags for the retrieval of valid common macro-pixels. This assessment is required in order to ensure the reliability of monitoring systems based on MERIS data, such as the Swedish coastal and lake monitoring system (http.vattenkvalitet.se). The results show that the pre-processing with the Improved Contrast between Ocean and Land (ICOL) processor, correcting for adjacency effects, improve the retrieval of spectral reflectance for all processors, Therefore, it is recommended that the ICOL processor should be applied when Baltic coastal waters are investigated. Chlorophyll was retrieved best using the FUB (Free University of Berlin) processing algorithm, although overestimations in the range 18–26.5 %, dependent on the compared pairs, were obtained. At low chlorophyll concentrations ($< 2.5\,\mathrm{mg\,m^{-3}}$), random errors dominated in the retrievals with the MEGS (MERIS ground segment processor) processor. The lowest bias and random errors were obtained with MEGS for suspended particulate matter, for which overestimations in te range of 8–16 % were found. Only the FUB retrieved CDOM (Coloured Dissolved Organic Matter) correlate with in situ values. However, a large systematic underestimation appears in the estimates that nevertheless may be corrected for by using a local correction factor. The MEGS has the potential to be used as an operational processing algorithm for the Himmerfjärden bay and adjacent areas, but it requires further improvement of the atmospheric correction for the blue bands and better definition at relatively low chlorophyll concentrations in presence of high CDOM attenuation.

1 Introduction

Coastal waters are recipients of high inputs of organic matter and nutrients from land, derived from natural processes and human activities (Borges, 2005). This matter and energy exchange between the open sea, coastal waters and land can be observed by changes in the spectra of the water-leaving radiance (L_w), which is perceived as water colour. The water colour varies according to the prevailing light and physical conditions at the sea surface and depends on the range of concentrations and optical properties of in-water constituents (Prieur and Sathyendranath, 1981; Mobley, 1994). Coastal waters rich in coloured dissolved organic matter (CDOM) represent a challenge for optical remote sensing. CDOM absorption (aCDOM) has a strong impact on the L_w in the visible short wavelengths, which highly influences satellite remote sensing data over in coastal and inland waters. The amount of L_w (443 nm) is approximately 9.8 % of total radiance (L_t) over open ocean waters measured at the top of atmosphere, while it is only about 0.4 % for CDOM-dominated waters (IOCCG, 2010). Furthermore, the absorption of CDOM near 443 nm corresponds to the chlorophyll *a* peak of phytoplankton absorption. The aCDOM, chlorophyll *a* concentration and suspended matter concentration are water quality parameters of interest for coastal management, and they can be derived from optical remote sensing, specifically from MERIS measurement.The dominance of aCDOM in the attenuation of light continues to be a challenge for chlorophyll *a* retrieval algorithms in ocean colour remote sensing (Carder et al., 1991; Nelson and Siegel, 2013).

In coastal waters, suspended sediment and dissolved organic matter usually do not co-vary with the chlorophyll *a* concentration (Morel and Prieur, 1977). Different combinations and concentrations of optical constituents may result in the same spectral reflectance signature measured by the sensors, making it difficult to interpret. This, in turn, may hinder accurate retrieval of absorption and scattering properties (i.e. inherent optical properties, IOPs) and subsequent retrieval of concentrations of optical water constituents.

Elaborate methods are required to derive the concentrations of optical variables accurately from space, e.g. matrix or neural network inversion (IOCCG, 2010). Different algorithms have been developed for this task which have been validated against in situ measurements and inter-compared. From those, the most common coastal processors that are distributed freely were used in this study. The standard MEGS processor (Case-2 water processing branch), the FUB/WeW processor developed by the Free University Berlin, here referred to as FUB (Schroeder et al., 2007a, b), the Case-2 regional processor C2R (Doerffer and Schiller, 2007) and the boreal water processor (BOREAL) (Doerffer and Schiller, 2008). Each of the above processors (including the Case-2 branch of MEGS) use a multiple non-linear regression method, i.e. Neural Network (NN) that includes simulations of radiative transfer models to derive the light propagation through the water and the atmosphere linked with bio-optical models. It must be noted that the FUB processor resolves the water products directly from top-of-atmosphere radiance, whereas the other three processors first derive the level 2 reflectance. The latter is then used to derive IOPs (absorption and scattering), which are subsequently used to derive the level 2 water products.

The combined use of satellites and in situ observations may maximize the benefits of ocean colour observations (Gregg and Conkright, 2001). Currently, only three satellite ocean colour sensors have about 10 yr of global coverage of data, i.e. SeaWiFS (1997–2011, NASA), MODIS (1999–on-going, NASA) and MERIS (2002–2012, ESA). MERIS was especially adapted to coastal applications. It had high spatial resolution (290 m × 260 m) and spectral resolution (15 spectral channels in the visible and near infrared region), compared to the other sensors (Doerffer et al., 1999; European Space Agency, 2011). However, the contact to the ENVISAT spacecraft was lost in April 2012, and hence transmission of MERIS data was no longer possible. The current focus of the ENVISAT mission is to encourage data exploitation of the 10 yr satellite data archive and to upgrade and validate image processing algorithms in order to derive the geophysical products (level 2 processing) accurately (Laur, 2012). This will lead to improved algorithms for the operational follow-up mission of MERIS, Sentinel-3 (the launch is planned in November 2014), which will carry the Ocean Land Colour Instrument (OLCI) that has improved characteristics compared to MERIS; e.g. a spectral resolution of 21 wavelength bands in the range 400–1020 nm.

Kratzer et al. (2008) had shown that the FUB processor was best for retrieving level 2 products from the Himmerfjärden area, including the NW Baltic Proper. The FUB has also been applied successfully in other areas of the Baltic Sea (Ohde et al., 2007; Vaičiūtė et al., 2012). Kratzer and Vinterhav (2010) showed that the retrieval of level 2 products over Swedish coastal waters was improved by using a combination of the Improved Contrast between Ocean and Land (ICOL) processor (Santer and Zagolski, 2007, 2009), correcting for adjacency effects, and the FUB processor. An independent end-user survey also tested the results of different processing schemes in coastal and lake areas (Philipson et al., 2009). All end-users confirmed that the images that had been processed with ICOL and FUB represented best the ranges of water quality parameters for the respective water body (Swedish great lakes and Himmerfjärden area) and season. The processing chain ICOL-FUB was therefore applied to the operational monitoring system (http.vattenkvalitet.se) for the Swedish great lakes and the coastal areas.

At the end of 2011, ESA completed the third reprocessing of the full MERIS archive. At that time a new version of ICOL was also made available (v. 2.9.1). Therefore, the previous results need to be reassessed in order to confirm that they are still valid, or if a change is required in the processing chain of the operational system in order to secure its reliability. Here, a study that assesses the most common MERIS processors for coastal waters (using MERIS 3rd reprocessing data against sea-truthing data) is presented. An increased number of match-up data was available, including data from the spring season (2010). This new study also includes the assessment of accuracy of aCDOM retrieval, which could not be performed before because of the lack of available in situ measurements of aCDOM (Kratzer and Vinterhav, 2010). Besides the further development of MERIS processing, the algorithm to retrieve the MERIS reflectance for the in situ radiometer (TACCS) used for validation was also improved. The aim of the present study is to make processing recommendations for the current monitoring system, based on MERIS data 3rd reprocessing, to identify the advantage of the different MERIS processors for the retrieval of water quality parameters in the Baltic Sea and, furthermore, to make recommendations for future satellite missions such as Sentinel-3, which is planned to be launched by ESA at the end of 2014.

2 Data and methods

2.1 Study area

The region of interest is on the north-western coast of the Northern Baltic Proper (Fig. 1), south of Stockholm archipelago, including Himmerfjärden bay and its adjacent areas, top-left latitude and longitude (60° N, 17° E) and bottom right coordinates (58° N, 19° E). This region is a brackish marine ecosystem (Elmgren, 2001). The influence of tides is negligible in most of the Baltic Sea, therefore the main circulation is driven by the surface wind speed and changes in atmospheric pressure (Leppèaranta and Myrberg, 2009). The Baltic Sea and Himmerfjärden are optically dominated by CDOM absorption (Kutser et al., 2009; Kratzer and Tett, 2009).

Himmerfjärden bay follows a regular phenology of phytoplankton blooms that occur in the Baltic Sea during spring and summer. The summer blooms are of special environmental and health interest because they are dominated by the potentially toxic nitrogen-fixing filamentous cyanobacteria, *Nodularia spumigena* and non-toxic *Aphanizomenom sp*. The chlorophyll *a* (Chl *a*) concentrations that can be observed within Himmerfjärden range from 1 mg m^{-3} up to 18 mg m^{-3}, with higher values during the spring bloom. The suspended particulate matter (SPM) load ranges from 0.5 g m^{-3} up to 2.7 g m^{-3} with decreasing values towards the open sea (Kratzer and Tett, 2009). The absorption of CDOM (g440) in Himmerfjärden ranges from 0.39 m^{-1} up to 1.27 m^{-1}, and in the open sea from about 0.3 m^{-1} to 0.5 m^{-1}. The Himmerfjärden region has a local catchment area of 536 km^2 receiving a minor freshwater outflow from Lake

Mälaren (Franzén et al., 2011). Located within the Himmerfjärden bay (Fig. 1) is the third largest sewage treatment plant in the Stockholm region. From 2007 to 2010 an adaptive management experiment was carried out in the Himmerfjärden sewage treatment plant (HSTP) to study the effects of nitrogen release on eutrophication and the development of cyanobacteria blooms. The experiment entailed effluent release without nitrogen treatment during 2007–2008, and with full capacity nitrogen treatment during 2009–2010.

2.2 Sea-truthing data

2.2.1 Water samples

The sea-truthing data was gathered during two monthly field campaigns in July 2008 and spring 2010 (with one additional transect in August 2008, Table 2). Water samples were taken through Himmerfjärden bay as well as along two transects off-shore. Usually, 3–4 sampling stations can be done per transect in one day (casts by date). The starting time for the sampling usually began 1–2 h before the MERIS overpass (Table 2). For the validation of satellite data water samples were taken from just below the surface using a sampling bucket. Concentrations of organic and inorganic SPM were measured by the gravimetric method (Strickland and Parsons, 1972). This method has an error of 10 % to derive total SPM in summer from surface water samples in the Baltic Sea (Kratzer, 2000). For the determination of aCDOM, the water was filtered through 0.2 µm membrane filters and measured spectrophotometrically in a 10 cm optical cuvette in a Shimadzu UVPC 2401 dual beam spectrophotometer. The optical density (OD), which is equivalent to absorbance at 440 nm, was corrected for the OD at 750 nm. The absorption at 440 nm was derived as described in Kirk (1994) and Kratzer (2000). For the estimation of chlorophyll *a* (Chl *a*), the trichromatic method was applied (Jeffrey and Humphrey, 1975; Parsons et al., 1984). The samples were filtered through GF/F filters and kept in liquid nitrogen until they were analysed. They were then extracted into 90 % acetone using sonication. The trichromatic method has an error of 7 % when deriving Chl *a* from Baltic Sea triplicates sampled in different bottles (Kratzer, 2000). During 2002, an international chlorophyll inter-calibration exercise was coordinated by the Norwegian Institute of Water Research (NIVA) for the European MERIS Validation Team (MVT) (Sørensen et al., 2007). The results of the MVT inter-calibration showed that the spectrophotometric Chl *a* measurements of natural water samples by the marine remote sensing group from Stockholm University were within 8.6 % of the median value of the international group. In previous tests the method to derive aCDOM had shown much less variability between replicates from different bottles (Kratzer, 2000), than for SPM and Chl *a*, and in this study it is assumed to be well below 5 %.

2.2.2 Field radiometry

The Tethered Attenuation Coefficient Chain-Sensor (TACCS, manufactured by Satlantic Inc., Canada) is an in-water radiometer deployed on a floating buoy. The TACCS has an in-water up-welling radiance sensor Lu(λ) with a full-angle field of view (FAFOV) of 20° at nominal depth 0.5 m. The Lu sensor has 7 channels matching the MERIS bands centred at 412, 443, 490, 510, 560, 620 and 665 nm. The TACCS includes an in-air downward irradiance sensor Ed centred at 443, 490 and 670 nm. The TACCS also includes an in-water chain of Ed($\lambda = 490$ nm) at the nominal depths of 2, 4, 6, and 8 m. All sensors have a 10 nm bandwidth. TACCS measurements are logged in three minutes intervals at an acquisition rate of 0.5 Hz and approximately at 20 m distance from the ship to avoid ship shading.

Coincident optical profiles were taken with the TACCS using an AC9+ from WET Labs, measuring spectral absorption *a* and beam attenuation *c* at 412, 440, 488, 510, 532, 555, 630, 676, and 715 nm as described in Kratzer et al. (2008). By using the TACCS and AC9+ data, the sea surface reflectance ρ_w in Eq. (1), can be calculated (Kratzer et al., 2008; Zibordi et al., 2012) and used for the validation of the MERIS

Title Page
Abstract Introduction
Conclusions References
Tables Figures
◀| |▶
◀ ▶
Back Close
Full Screen / Esc
Printer-friendly Version
Interactive Discussion

reflectance data. The TACCS processor is also described in the MERIS optical measurements protocols Barker (2011).

$$\rho_{\mathrm{w}}(\lambda) = \frac{\pi \times L_{\mathrm{u}}(0^{+},\lambda)}{E_{\mathrm{s}}(\lambda)} \tag{1}$$

Where L_{u} is the spectral upwelling radiance interpolated just above the surface (0^{+}) and E_{s} is the down welling incident spectral irradiance.

During each field campaign, quick-looks of the Advanced Very High Resolution Radiometer (AVHRR) data from the Swedish Meteorological and Hydrological Institute (SMHI) were used to specifically avoid surface accumulations of cyanobacteria in order to assure minimum horizontal optical heterogeneity of the water body. Furthermore, daily meteorological forecasts were used for planning the sea-truthing campaigns and for avoiding transect days with high wind speeds and/or cloudy conditions. Here, it is assumed that the natural spatial and temporal variability of the sea surface reflectance remains without significant changes for the selected time window of the match-up with the satellite.

A prototype processor to derive reflectance from TACCS data was described in Kratzer et al. (2008) and used for the validation of reflectance data in Kratzer and Vinterhav (2010). During 2010–2012, a new TACCS processor was developed in order to improve the retrieval of reflectance and to describe the uncertainties involved (Moore et al., 2010; Zibordi et al., 2012), which allows an improved assessment of MERIS data against sea-truthing measurements. In this study, the latest processor as described in Zibordi et al. (2012) and the respective calibration files were used to process the TACCS data from both years 2008 and 2010.

2.3 Satellite data processing considerations

2.3.1 Level 1b processing

Prior to field campaigns, the overpass times of ENVISAT were predicted by using the Earth observation swath and orbit visualization tool-next generation software (ESOV-NG version 2.0). These dates were then used for the booking of ship time for validation against in situ measurements. A dataset consisting of 14 MERIS full resolution (FR) level 1b scenes (3rd re-processing) were acquired for the study area that coincided with the field measurements of two sea-truthing campaigns (Table 2). The time difference between in situ measurements and the MERIS overpass was less than two hours for most of the stations investigated here.

The accurate MERIS ortho-rectified geo-location operational software (AMORGOS-version 4.0p1) was used to improve the location accuracy in the level 1b MERIS dataset. AMORGOS improves the geo-location of MERIS FRS products by using accurate satellite attitude and orbit files and the GETASSE 3.0 Digital Elevation Model (DEM) to generate three new bands, latitude, longitude and altitude for each MERIS pixel which results in a MERIS product mode called full swath geo-corrected (FSG) (ACRI-ST, 2011). The AMORGOS tool was also used in this study for sub-setting the MERIS datasets. The total number of lines to process was reduced to 577 with AMORGOS. This is a clipping operation over the region of interest which serves two purposes, (1) it preserves the ENVISAT file format (.N1 file) as required by the ODESA CFI software (ACRI-ST, 2012) and, (2) it facilitates the application of the ICOL processor to correct for adjacency effects (Santer and Zagolski, 2009) by using a smaller image size, and also preserves the ENVISAT file format.

The MERIS FSG datasets were then batch-processed using the graph processing framework (GPF) of the Earth Observation Toolbox and Development Platform (BEAM, version 4.10.3) software. A cloud mask was generated for the MERIS FSG dataset using BEAM with the cloud probability processor version 1.5.203 including the advanced land-water mask. The cloud probability processor uses two artificial neural nets that provide a cloud probability value in the range of 0–1. The pixel value is set as cloudy when the probability value > 80 %, cloud free (probability < 20 %) or where it is uncertain (20 % < probability < 80 %).

The level 1b dataset, using standard procedures, was also corrected for systematic radiometric differences within the detector of the five cameras that cover the swath of the MERIS FRS images to reduce the "vertical striping" by radiometric equalisation of coherent noise (Bouvet and Ramino, 2010). The satellite data were also corrected for the variations of the spectral wavelength of each pixel along the image, the so-called "smile effect" correction, resulting in a reduction of disturbances at camera borders (MERIS_ESL, 2008). The smile correction (SC) and the equalization of coherent noise (EQ) are implemented in the MERIS level 1b radiometry correction operator version 1.1 available in BEAM.

The land adjacency effects in the study area were corrected for by using the ICOL 2.9.1 processor. Two MERIS level 1b processed datasets were then produced. Both datasets included the SCEQ corrections as default, but only one dataset was ICOL corrected. This study will use the acronym "L1N" to indicate that ICOL has been applied. Furthermore, a separate MERIS level 1b dataset was kept for further processing with the MERIS Ground Segment Development Platform (MEGS) standard level 2 processor version 8.1. This dataset includes only EQ correction with and without ICOL. The smile correction was not applied to the input data for MEGS, because MEGS includes the smile correction as a default. Table 1 shows the level 1b processing schemes used for the MERIS datasets comparison.

2.3.2 Level 2 processing

The standard MEGS processor (Case-2 water processing branch) and three coastal processors that are provided as source free plug-ins for the BEAM software, were used to derive the geophysical products (level 2 processing). The FUB processor (Schroeder et al., 2007a, b). The Case-2 regional processor C2R (Doerffer and Schiller, 2007) and boreal lakes water processor BOREAL (Doerffer and Schiller, 2008).

The processors assume environmental conditions as: infinite deep water with vertical homogeneous distribution of water constituents; no inelastic scattering or polarization effects are considered. The derived geophysical products for each processor used for the evaluation included algal pigments considering chlorophyll *a* as proxy for biomass, here referred to as CHL, suspended particular matter (SPM) and aCDOM. The radiometry measured in situ is limited to the first 7 bands of MERIS. Therefore, only the MERIS reflectance $\rho_w(\lambda)$ at 412, 443, 490, 510, 560, 620 and 665 nm estimated by each processor was used in this study. The ranges of concentrations of optical properties used for training the FUB processor are described in Schroeder et al. (2007b); Zhang (2003). The range of optical properties parameterizing MEGS and C2R are given in Doerffer and Schiller (2007); Doerffer (2011). The parameterization range for BOREAL can be found in Koponen et al. (2008). The concentration ranges of the respective processors are summarized in Table 3.

2.4 Macro pixel quality and exclusion criteria

Along the Swedish coast the typical current velocity in the Baltic Sea ranges from 2 to $5\,\mathrm{cm\,s^{-1}}$ (Maslowski and Walczowski, 2002). Considering the $5\,\mathrm{cm\,s^{-1}}$ to be a fast moving current in the study area, the water mass may move maximum 180 m in one hour, and in two hours the water mass may thus move about one MERIS pixel. A matrix of 3 × 3 pixels centred at the field sample location has been used to cover the natural variability of water displacement. Therefore, only those casts that were sampled during a match-up time window within the satellite overpass of 2 h or less (Table 2) have been selected for validation.

Each processor can raise flags at different stages of processing. These flags provide additional information regarding surface type (i.e. land, water, cloud); they also provide confidence information when the algorithm input or output is outside the expected range. Therefore, the macro pixels that represent water were filtered by flags, and pixels within the macro pixel were excluded if a flag was raised according to Table 5 (note that for geophysical products different terms are used by different authors and here the nomenclature was standardised for consistency throughout the paper, i.e. CHL for algal_2 and chl_conc; SPM for total_susp and tsm; aCDOM for yellow_subs and a_y_443). Only macro pixels with 5 or more non-flagged pixels were kept for further analysis and their pixel values were averaged (Kratzer and Vinterhav, 2010). The value of each macro pixel was assumed to represent the local conditions of the station cast for a given date. Due to the horizontal heterogeneity caused by the cyanobacteria blooms a certain degree of variability within macro pixels is to be expected. Furthermore, coastal processes, fronts and natural gradients that may occur in the water body also add to this natural variability in the coastal zone. Nevertheless, after applying the exclusion criteria, the macro pixels were considered to have minimum horizontal heterogeneity for coastal conditions and obviously do not represent oligotrophic conditions. Therefore, the homogeneity test proposed by Bailey and Werdell (2006) to minimize the impact of geophysical variability within the macro pixels were modified to derive only those pixels after being filtered by the quality flags and minimum required pixels. The bias was calculated by using the standard deviation of the remaining “viable” pixels, this represents the minimum error that relates to the natural variability within the 3 × 3 pixel window.

Each processor may result in a different set of viable macro pixels. In order to ensure that all water quality estimates from the different processors compare the same pixels only those pixels that are common within a viable macro pixel for each processor were used to derive the macro pixel averaged value for comparison. For the radiometry only common macro pixels between all processors were used to assess the differences. For water products common macro pixels for each product among the pair of processors being compared are used for the analysis. This maximizes the number of viable macro pixels available for the differences estimates and ensures a fair comparison between the processors, i.e. the processors deals with the same pixels and observing conditions to derive the respective geophysical products.

Title Page
Abstract Introduction
Conclusions References
Tables Figures
◀◀ ▶▶
◀ ▶
Back Close
Full Screen / Esc
Printer-friendly Version
Interactive Discussion

2.5 Comparison of MERIS-derived data products with in situ measurements

For each processor the derived MERIS reflectance $\rho_{\mathrm{w}}(\lambda)$ from the ICOL-based processing scheme (SCEQ_L1N) and non-ICOL processing (SCEQ_X) were compared against the in situ TACCS data. Common macro pixels among the two processing schemes were selected and the sum of absolute differences against in situ data (SABS_D, Eq. 2) were calculated. These were then used to estimate the percentage of change between the two processing schemes (Δ_{ICOL}, Eq. 3). Here, the SCEQ_X processing was used as a reference to evaluate the direction of change. A negative value of the Δ_{ICOL} indicates a reduction of SABS_D for the SCEQ_L1N processing.

$$\mathrm{SABS\_D} = \sum_{i=1}^{n_{\mathrm{casts}}} \left| \rho_{\mathrm{w}}(\lambda)_i^{\mathrm{MERIS}} - \rho_{\mathrm{w}}(\lambda)_i^{\mathrm{TACCS}} \right| \tag{2}$$

$$\Delta_{\mathrm{ICOL}} = \frac{(\mathrm{SABS\_D}_{\mathrm{SCEQ\_L1N}} - \mathrm{SABS\_D}_{\mathrm{SCEQ\_X}})}{\mathrm{SABS\_D}_{\mathrm{SCEQ\_X}}} \times 100 \tag{3}$$

The validation was done over the datasets that had improved the MERIS reflectance for each processor. The ICOL-processed datasets (SCEQ_L1N) were the basis of the water products (CHL, SPM and aCDOM) validation, i.e. all level 2 products were smile corrected, equalized and a test on ICOL was done. It was tested that the ICOL-processed data had worked as expected (i.e. reducing the land adjacency effects when the pixels are closer to the coast) and statistical evidence was gathered that it had substantially improved the MERIS reflectance retrieval for each processor. The datasets derived from SCEQ_L1N were then used to assess the differences in $\rho_{\mathrm{w}}(\lambda)$ retrieval amongst processors compared to in situ data.

Pair-wise comparison of the mean values of viable macro pixels to in situ data were then used for the analysis. Differences were quantified statistically by using the Mean Normalized Bias (MNB, Eq. 4) which is an estimate of systematic errors; the Root Mean Square of Relative Differences ($\mathrm{RMS}_{\mathrm{RD}}$, Eq. 5) that indicates random error in the retrieval.

$$\mathrm{MNB} = \mathrm{mean}\left[\frac{y_i^{\mathrm{MERIS}} - x_i^{\mathrm{insitu}}}{x_i^{\mathrm{insitu}}}\right] \times 100 \tag{4}$$

$$\mathrm{RMS_{RD}} = \mathrm{stdev}\left[\frac{y_i^{\mathrm{MERIS}} - x_i^{\mathrm{insitu}}}{x_i^{\mathrm{insitu}}}\right] \times 100 \tag{5}$$

Where $i = 1, \ldots$ number of averaged macro pixels and, mean and stdev, referred to the calculations of the mean and standard deviation value, respectively.

3 Results

The observed range of in situ concentrations of Chl *a*, SPM and aCDOM for the two sea-truthing campaigns is presented in Table 4. The median chlorophyll concentration measured in situ was about 2.7 mg m^{-3}, the median SPM concentration was about 1.3 g m^{-3} and the median g440 (CDOM absorption at 440 nm) was 0.4 m^{-1}. The sea-truthing data were found within the training ranges of the used level 2 processors (Table 3). The in situ Chl *a* and SPM had a positive correlation, $r = 0.74$ (data from 2008 and 2010, Fig. 2. Low correlation values were found for aCDOM vs. Chl *a* ($r = 0.02$) and aCDOM vs. SPM ($r = 0.18$) when the cast ID H4_6a is excluded as this single value was identified as outlier of normal conditions (data from 2010 only, as there were no aCDOM data for 2008).

During 2008, the inner stations of Himmerfjärden were highly influenced by the release of nitrogen from the Himmerfjärden sewage treatment plant (HSTP). Higher SPM and aCDOM values observed in 2010 at the station H4 (cast ID: H4_6a, Table 2). This suggests that the location of H4 may optically be strongly influenced by the effluent outflow of the Himmerfjärden sewage treatment plant.

The ranges of optical properties differed sustantially for the two sea-truthing campaigns in 2008 and 2010. A higher Chl *a* and SPM range of concentrations were observed in 2008. A smaller range of Chl *a* and SPM values were found for the sea-truthing data in 2010 (during full nitrogen treatment), whilst data from 2008 (no nitrogen treatment) generally had a greater range of values and were more variable. Station H5_3a in 2008 (Fig. 2) was found to be an outlier with the highest Chl *a* and SPM values. This was during a strong cyanobacteria bloom in which usually the relationship between satellite data and truthing data breaks down because of strong patchiness of the water body and strong horizontal heterogeneity, making it difficult to compare the satellite retrievals to truthing data. Water transparency as measured by Secchi depth showed less transparent waters in 2008 with an average of 4.42 ± 1.56 m compared to 6.45 ± 1.65 m in 2010. In 2008, a Secchi depth minimum value of 1.9 m was observed at station H5, with Secchi depths increasing towards the outer Himmerfjärden stations. The Secchi depth was not found to be above 3 m in 2008 for the inner stations H5 and H4; Station H3 showed a Secchi depth range of 2.9–3.5 m and for H2 Secchi depth ranged between 3.4 and 4.1.

3.1 MERIS reflectance evaluation

For MEGS and FUB, the use of ICOL increased the number of viable macro pixels that previously had been flagged by the macro pixel quality and exclusion criteria applied. MEGS available macro pixels without ICOL were 17, and after ICOL there were 24 macro pixels, i.e. an increase of 41 % of viable pixels. The ICOL viable macro pixel retrieval ratio for FUB was 19/14, an increase of 35 %. For the locations H2 and H3, only FUB could reliably retrieve the reflectance. The viable macro pixel retrieval ratio was 27/27 for both C2R and BOREAL. Based on these results, the ICOL-based datasets were used for the following comparison of level 2 products derived from all processors. Common macro pixels used to evaluate the retrieval of $\rho_w(\lambda)$ resulted in 16 common macro pixels among the 4 processors after macro pixel quality control and exclusion criteria using the SCEQ_L1N datasets.

In general, FUB and MEGS estimates showed systematic errors, thus, an underestimation of $\rho_w(\lambda)$ showed up in all bands compared to sea-truthing data (Table 6). The

FUB processor underestimated $\rho_w(\lambda)$ between 22 % and 32 %, while MEGS underestimates by 7–16 % in the spectral bands above 443 nm. For the MEGS estimates of $\rho_w(\lambda)$ the highest underestimation (35 %) were found at 413 nm. On the other hand, an overestimation was found for C2R for the blue spectral bands, while the lowest systematic errors occur for the green spectral bands at 510 and 560 nm (1.1 % and 8 %, respectively) for this processor. It may be pointed out that the highest uncertainty in the TACCS estimates occurs in the red channels (Zibordi et al., 2012), but the satellite retrieval amongst processors was most consistent in the red.

The $\rho_w(\lambda)$ estimates showed relatively low correlation in the blue bands 413 and 443 nm for all processors (Table 6). The correlation coefficient of $r = 0.11$ for FUB at 413 nm were the lowest amongst all processors. The best correlation with in situ values, with r values above 0.84 for all processors and as high as 0.91 for MEGS, was found for the 560 nm wavelength (Fig. 3, Table 6). For $\rho_w(\lambda = 560)$ an underestimation and increase of variability higher than 0.015 was observed.

3.2 CHL evaluation

In general, all processors overestimated the CHL concentration. FUB was found to have the lowest systematic and random errors (Table 7). FUB showed an overestimation of chlorophyll of about 18–27 %, depending on the compared pairs after macro pixel exclusion criteria. MEGS showed an overestimation of 57–62 %. The random errors of FUB were consistent among pairs with $\mathrm{RMS_{RD}}$ values not higher than 55 %, while C2R random errors varied among pairs and were above 104 %. MEGS random errors were intermediate between 77 % and 87 %. BOREAL presented the highest systematic and random errors in all pairs (Table 7). FUB showed less variability at lower CHL concentrations (e.g. $< 4\,\mathrm{mg\,m^{-3}}$, Fig. 4a) than C2R and MEGS.

3.3 SPM evaluation

The MEGS processor was most accurate in retrieving SPM, while systematic overestimations were obtained with the MEGS, C2R and BOREAL processors. Only with the FUB processor the SPM loads were underestimated in all compared pairs (Table 8). When compared with FUB a MNB of only about 8 % was obtained with MEGS, whereas an underestimation of 28 % was found for the FUB processor. The C2R retrievals were also satisfying when the processor was compared (pairwise with FUB and MEGS) to in situ measurements (5.5 and 25.21 %, respectively). Random errors expressed by the $\mathrm{RMS}_{\mathrm{RD}}$ were mainly found in the range of 40–50 % among all processors, with the exception for BOREAL. The BOREAL estimates showed the highest random errors with values above 60 %.

The retrieved SPM concentrations by MEGS are associated with significant random errors, while small systematic bias (Table 8) are obtained when compared to FUB (Fig. 4b). The C2R and MEGS estimates are relatively close to the 1 : 1 line, covering a wider range of in situ concentrations. The MEGS retrievals have the lowest systematic bias and random errors (Table 8).

3.4 aCDOM evaluation

All processors underestimated aCDOM (Table 9). MEGS and C2R were not able to resolve the in situ aCDOM distribution as all the retrieved macro pixels estimated similar aCDOM values (Fig. 5). FUB was able to resolve changes in aCDOM, albeit with a systematic underestimation when compared to in situ values. Figure 6 shows the regression equation obtained between FUB retrieved and in situ measured aCDOM that can be used as local correction factor in order to improve the aCDOM retrieval. However, it must be noted that this factor will only be valid for the range of concentrations investigated here.

The results confirm the challenges to estimate aCDOM in the Baltic Sea accurately when a limited dataset is applied to the present processors. In this study, 17 in situ aCDOM samples from 2010 were available for satellite validation. As mentioned before, the aCDOM field measurements for 2008 were not available. After applying the macro pixel quality control and exclusion criteria during the pairwise combination, a reduced number of macro pixels were available to perform the comparisons with in situ data. The pairwise combination of C2R vs. FUB showed the maximum available pixels, with only 7 macro pixels left. The quality control of BOREAL when common macro pixels are used in the pairwise comparison left only one or two viable pixels to make such comparisons, making it impossible to evaluate.

3.5 CHL and SPM evaluation by year

Using all available individual macro pixels for FUB ($n = 26$, 16 and 10 observations in 2008 2010, respectively), the CHL retrievals (Table 10) showed lower systematic errors for 2008 than 2010 (MNB = 16 % and 24 %, respectively). Random error obtained with the FUB processor was higher for 2010 than 2008 (108 % and 61 %, respectively). Systematic errors of 57 % and 56 % were obtained with the MEGS processor for 2008 and 2010, respectively. Using MEGS, the total number of retrieved macro pixels for CHL was 21 (15 observations in 2008 and 6 observations in 2010). Random errors were above 69 % for both years (RMS_{RD} 70 % and 102 %, 2008 and 2010 respectively). Suspended particulate matter showed the lowest systematic and random errors in 2010 than in 2008 (MNB = −1 %, $\text{RMS}_{\text{RD}} = 43$ %) using MEGS (Table 10). FUB was underestimated SPM in both years up to 47 %. The C2R processor was the only processor retrieving the same amount of number of macro pixels regardless of the water product ($n = 27$). FUB and MEGS retrieved less individual macro pixels for SPM than for CHL (macro pixels ratio SPM/CHL 19/26 FUB and 15/21 for MEGS).

In order to obtain a fair comparison of the performance of FUB and MEGS by using the individual macro pixel a subset of macro pixels dataset was used. Station H5 was removed from the FUB dataset, as it drives the correlation of CHL vs. sea-truthing for 2008 and may add a clear bias to the results as this station was not retrieved by MEGS after the macro pixel quality and exclusion criteria were applied for the same year. Furthermore, the open sea stations CI, CII, CIII that are in a different sub-catchment and represent a different water body than the stations within and close to the Himmerfjärden bay, were therefore also removed from the comparison.

Higher ranges of CHL values and variability was observed during 2008 than in 2010, for both processors (Table 11). MEGS had lower systematic errors in 2008 (MNB = 23.1 %) and reduced random errors ($\mathrm{RMS_{RD}}$ = 36.9) than FUB (MNB = 28.5; $\mathrm{RMS_{RD}}$ = 37.1). However, in 2010 the opposite performance occurred for MEGS (MNB = 55.8; $\mathrm{RMS_{RD}}$ = 102.0), FUB being more accurate (MNB = 24.1; $\mathrm{RMS_{RD}}$ = 108.2).

Suspended particulate matter systematic errors and random errors in FUB and MEGS remained without change after the subset of individual macro pixels. The inner stations within Himmerfjärden show a higher discrepancy to the sea-truthing data in 2008 for both processors.

Nevertheless, caution is advised in the interpretation of results using individual macro pixels because they cannot be directly compared between FUB and MEGS, they represent their individual best, and they may not share the same observed macro pixels (as it was done in the previous sections), thus they are likely to show discrepancies because the same pixels may not be compared. However, this comparison highlights the processor individual performance and its potential limitations within Himmerfjärden and adjacent areas.

4 Discussion

The results from the processors have shown less accurate $\rho_w(\lambda)$ retrievals in the blue spectral region and better agreement in the green-red spectral region, similar to other optically-complex coastal water bodies (Park et al., 2004). Relative low $\rho_w(\lambda)$ in situ values in the blue bands 413 and 443 can be expected as the optical properties of the Baltic Sea are dominated by aCDOM (Schwarz et al., 2002; Darecki and Stramski, 2004; Reinart and Kutser, 2006) and SPM is low (Park et al., 2004).

FUB has a rather consistent off-set over the whole reflectance spectrum (Table 6), and has therefore the most consistent spectral shape, i.e. the MNB do not change as drastically as for the other processors. MEGS has shown lower systematic errors than FUB (Table 6) for all wavelengths but 413 nm when using the standard MERIS reflectance considering the Case 1 water branch. This is notable for MEGS over optically-complex waters, and suggests a further improvement of the standard radiometric products when ICOL is applied.

Differences in CHL and SPM retrievals by MEGS and C2R were observed. However, the MEGS case 2 branch and the C2R share not only the same architecture, but the water and atmospheric nets used in their bio-optical model are also the same (at least for processors versions used here for MEGS 8.1 and C2R 1.5.3, personal communication, Mazeran, C., 2013). Therefore, these differences may arise in the implementation of pre-corrections of the TOA signal (e.g. smile and gaseous corrections) and in the use of predefined physical constants (i.e. the solar flux at theoretical wavelengths) that may scale up in the level 2 water products.

Lower in situ chlorophyll concentrations (mainly $< 2.5\,\mathrm{mg\,m^{-3}}$, Fig. 4) seem to have an influence on the accuracy. FUB is more stable and accurate especially in the open Baltic Sea, while MEGS and C2R showed greater variability. This higher variability is expressed in C2R and MEGS as an overestimation with higher random errors in the retrieval. Low performance of the neural network processors occurs when decreasing pigment concentrations in waters dominated by CDOM absorption, as aCDOM and SPM become the dominate optical signals (Doerffer and Schiller, 2007). These differences may also be linked to the relatively small ranges of in situ SPM and Chl *a* concentrations in comparison to the higher range of the processors, combined with relatively high aCDOM. As a consequence, in MEGS and C2R, low chlorophyll concentrations may be overestimated, while higher concentrations may not be overestimated. This may lead to a reduced difference between higher and lower pigment concentrations. An expression of this effect may be a reduced contrast of the image over the same range of values in comparison to FUB.

Furthermore, Heim et al. (2008) mentioned that by using the C2R in optically complex waters the main attribution of the total absorption goes towards the pigment absorption, leading to an overestimation of CHL at low chlorophyll concentrations and hence an underestimation of aCDOM. This is consistent with findings of Attila et al. (2013); González Vilas et al. (2011). Attila et al. (2013) have also shown that C2R retrievals in the Baltic Sea can be improved by modifying the mean conversion factors of the specific inherent optical properties, SIOPs (i.e. the chlorophyll conversion factor and exponent) used to derive the chlorophyll concentration from the absorption of phytoplankton pigments by using appropriate regional factors.

FUB showed lower accuracies for SPM retrievals than MEGS and C2R. These underestimations occurred mostly within Himmerfjärden, for the stations H3, H4 and H2 of the 18 July 2008 and 15 July 2008 datasets. The atmospheric correction in MEGS was more accurate for these cases than FUB and C2R.

Another potential cause of FUB SPM underestimations for stations not affected by atmospheric correction problems may be linked to the relatively small ranges of in situ SPM concentrations in comparison to the much higher range of the processor, combined with relatively high aCDOM in Baltic Sea waters. The underestimation of $\rho_w(\lambda)$ in the green band (560 nm) combined with a higher variability above > 0.15 seemed to affect FUB retrieval. The spectral band at 560 nm is related to the type and concentration of particulate material present in the water column which contributes to the absorption and backscattering of light. A highly variable distribution of particles affects the $\rho_w(\lambda)$ in the coastal zone (Stramski et al., 2004; Roesler and Boss, 2008). As the particle concentrations increase (including phytoplankton cells, organic particles, and detrital particulates) the backscattering increases, but parallel to this, the absorption may increase due to high aCDOM. Different phytoplankton communities may also affect the size and shape of the backscattering signal. Cyanobacteria have highly reflective gas vacuoles for regulating their buoyancy. Furthermore, they form dense aggregations (packaging effect) having a non-uniform distribution vertically and horizontally affecting both the absorption and scattering ratios (Kutser, 2004).

The individual macro pixels evaluation for FUB and MEGS showed some limitations in the performance of both processors. The truthing data showed that within Himmerfjärden Secchi depth was reduced and highly variable in 2008. Higher dissolved and suspended matter may have been released into the bay during lack of nitrogen treatment inducing the stimulation of primary production by increased release of the nutrients from Himmerfjärden Sewage plant. Water transparency was therefore decreased. CDOM absorption may also have been increased beyond the limit of aCDOM range for FUB as indicated by the high absorption measured by the AC9 and also by increased $K_d(490)$ values which are highly correlated to aCDOM. Vaičiūtė et al. (2012) found Secchi depth strongly correlated to aCDOM and SPM, and being the most influential factors explaining the discrepancies between MERIS-derived products and in situ data for Lithuanian coastal waters. High values of organic SPM during summer indicate the occurrence of cyanobacteria blooms, which may also add to the decreased light transmission indicated by lower Secchi depths. In Baltic Sea waters, it is usually aCDOM that is the dominant optical component influencing Secchi depth, but it is known to be less variable over space and time than SPM (Kratzer and Tett, 2009), SPM contributing more to the variability in Secchi depth.

FUB showed the highest discrepancies for the stations where Secchi values < 3.5 m were measured for both CHL and SPM. Random errors seems to dominate the retrieval of FUB CHL within Himmerfärden bay (Table 11). MEGS performed better in 2008 for CHL (i.e. at high chlorophyll ranges) and it seems to be able to retrieve higher CHL concentrations with high attenuation background. Although the sample size is very small, these results are consistent with the findings of Vaičiūtė et al. (2012) for the offshore area and in the plume area of the Curonian lagoon where even more turbid waters and higher aCDOM can be found. The authors found that the MERIS standard processor provided the best fit when compared to sea-truthing data. However, FUB was shown to flag less data than the standard processor (only 10 % of data were removed by FUB flags, whereas the standard processor removed 60 % of the match-ups). In this study, FUB also flagged less data than MEGS as can be seen for number of observations in the subset dataset for 2010 (FUB $n = 10$, MEGS $n = 6$, Table 11). FUB seems to have better agreement with sea-truthing data at low CHL values (e.g. $< 4\,\mathrm{mg\,m^{-3}}$) and with lower variability for open sea stations. FUB SPM retrievals were mostly underestimated (Table 11) which may be related primarily to atmospheric variability and clouds. The training data set in FUB, may not be representative for for the natural patterns of SPM occurring in the region of interest, as the data set used for training the neural nets were from the COASTLOOC project (Babin, 2000) representing more frequently waters with higher SPM. Furthermore, the inner stations remain underestimated for SPM and CHL using FUB, which may also suggest atmospheric correction failure (Cristina et al., 2009; Kratzer et al., 2008) not detected by the water flags in FUB, combined with adjacency effects that may limit the accuracy of SPM and CHL retrieval within Himmerfjärden. MEGS was able to retrieve SPM at lower concentrations than FUB for 2010, but MEGS may also be strongly affected by failure of atmospheric and/or adjacency correction for the inner stations in the bay (Table 11).

Further, the study of Sørensen et al. (2007) showed uncertainty of 5–20 % for deriving CHL with the spectrophotometric method in an international intercomparison between laboratories. Taking this into account, the overall accuracies obtained in this study, using FUB and MEGS for retrieving CHL from natural phytoplankton in coastal waters can be considered satisfying with regards to systematic errors. In the pairwise retrieval, chlorophyll was retrieved best using FUB with an overestimation between 18–26.5 % (MNB) and with a MNB of −29 % (2008) and 24 % (2010) in the individual FUB-sea-truthing comparison, which means that CHL can be derive within 30 % systematic error. The error of measuring SPM for the sea-truthing method used here is about 10 % in situ, and the pairwise retrieval showed MNB errors of 8–16 % for MEGS and −28 to −37 for FUB in this study. However, the previous study by Kratzer and Vinterhav 2010 had shown better SPM retrieval for FUB using MERIS data from the 2nd reprocessing with MNB −4 % in the open sea, and −15 % inside Himmerfjärden). For MEGS MNB was −22 % in the open sea, and −12 % inside Himmerfjärden.

5 Conclusions

The use of MERIS full resolution Level 1b 3rd reprocessing data in coastal waters rich in CDOM, with additional corrections for smile, equalization of coherent noise and correction of the adjacency effect using ICOL, has shown to improve the accuracy of the MERIS reflectance and derived water products, when compared to sea-truthing data. This processing sequence has further increased the number of viable quality pixels. Therefore the processing chain with ICOL processing is recommended to be applied in coastal Baltic Sea waters.

Overall, all investigated processors overestimate CHL values. Suspended particulate matter is retrieved better by all processors than the other water constituents. In the inversion process aCDOM strongly competes with CHL absorption causing aCDOM to be underestimated, and this may also affect CHL and SPM retrievals.

FUB is more accurate in the retrieval of CHL. In MEGS random errors dominate the retrievals at low chlorophyll $< 2.5\,\mathrm{mg\,m^{-3}}$.

MEGS is more accurate for SPM retrieval. FUB showed the highest discrepancies in SPM concentrations for stations with high atmospheric variability and where high Secchi depth $< 3.5\,\mathrm{m}$ were measured.

The choice of whether to use FUB or MEGS for retrieval of SPM in a given area of the Baltic Sea must be assessed against local conditions and ranges of optical components.

For future algorithms development in waters affected by high CDOM absorption it is therefore recommended to decouple the aCDOM retrieval from the retrieval of the CHL absorption at 443 nm (where high absorption of both aCDOM and CHL coincide), and instead, to use other spectral features of phytoplankton pigments in the longer wavelengths for chlorophyll retrieval, e.g. the chlorophyll peak in the red at about 665 nm.

Furthermore, the application of regional mean conversion factors SIOPs is recommended for potential improvements of MEGS or C2R before suggesting a processing change in the operational system. Although MEGS has already shown potential to be

Title Page
Abstract | Introduction
Conclusions | References
Tables | Figures
◀| |▶
◀ ▶
Back | Close
Full Screen / Esc
Printer-friendly Version
Interactive Discussion

used as operational processor in the Himmerfjärden bay and adjacent areas, it requires further improvement of the atmospheric correction for the blue bands and better definition at relatively low chlorophyll concentrations in presence of high CDOM absorption.

Acknowledgements. This research was funded by the Swedish National Space Board (Dnr. 99/09) and the European Space Agency (contract no. 21524/08/I-OL). The authors would like to thank the staff at Askö Laboratory for support during field work. Great thanks to Gerald Moore for further developing the TACCS processor and advice on radiometric measurements and calibrations. Thanks to the ODESA forum community, especially to Constant Mazeran, for valuable discussions and clarifications regarding the MEGS processor and Thomas Schroeder for answering questions regarding the architecture of FUB. Acknowledgements to Helena Höglander, Therese Harvey and Ragnar Elmgren from Stockholm University, Ecology, Environment and Plant Sciences, for valuable contributions regarding the Swedish National Monitoring Data and descriptions of the Himmerfjärden Sewage treatment plant nitrogen experiments. Thanks to and ACRI-ST for developing ODESA, available at http://earth.eo.esa.int/odesa.

References

ACRI-ST: The AMORGOS MERIS CFI (Accurate MERIS Ortho-Rectified Geo-location Operational Software) Software User Manual & Interface Control Document, pO-ID-ACR-GS-0003, 2011. 2166

ACRI-ST: ODESA software distribution, Quick start guide, ODESA-ACR-QSG, 2012. 2166

Attila, J., Koponen, S., Kallio, K., Lindfors, A., Kaitala, S., and Ylöstalo, P.: MERIS Case II water processor comparison on coastal sites of the northern Baltic Sea, Remote Sens. Environ., 128, 138–149, available at: http://www.sciencedirect.com/science/article/pii/S0034425712002817, 2013. 2178

Babin, M.: COAstal Surveillance Through Observation of Ocean Colour (COAST-LOOC), Final Report, Project ENV4-CT96-0310, 2000. 2180

Bailey, S. W. and Werdell, P. J.: A multi-sensor approach for the on-orbit validation of ocean color satellite data products, Remote Sens. Environ., 102, 12–23, doi:10.1016/j.rse.2006.01.015, 2006. 2169

Barker, K.: MERIS Optical Measurement Protocols, Part A: In situ water reflectance measurements, CO-SCI-ARG-TN-008, 2011. 2165

Borges, A. V.: Do we have enough pieces of the jigsaw to integrate CO_2 fluxes in the coastal ocean?, Estuaries, 28, 3–27, doi:10.1007/BF02732750, 2005. 2159

Bouvet, M. and Ramino, F.: Equalization of MERIS L1b products from the 2nd reprocessing, Tech. Rep. ESA TN TEC-EEP/2009.521/MB, ESA, 2010. 2167

Carder, K. L., Hawes, S. K., Baker, K. A., Smith, R. C., Steward, R. G., and Mitchell, B. G.: Reflectance model for quantifying chlorophyll *a* in the presence of productivity degradation products, J. Geophys. Res.-Oc., 96, 20599–20611, doi:10.1029/91JC02117, 1991. 2159

Cristina, S. V., Goela, P., Icely, J. D., Newton, A., and Fragoso, B.: Assessment of the water-leaving reflectances of the oceanic and coastal waters using MERIS satellite products in Sagres off the southwest coast of Portugal, J. Coastal Res., 1479–1483, available at: http://hdl.handle.net/10400.1/1106, 2009. 2180

Darecki, M. and Stramski, D.: An evaluation of MODIS and SeaWiFS bio-optical algorithms in the Baltic Sea, Remote Sens. Environ., 89, 326–350, doi:10.1016/j.rse.2003.10.012, 2004. 2176

Doerffer, R.: ATBD 2.255. Alternative Atmospheric Correction Procedure for Case 2 Water Remote Sensing using MERIS, Algorithm Theoretical Basis Document (ATBD) Version 1.0, Helmholtz-Zentrum Geesthacht, Geesthacht, 2011. 2168

Doerffer, R. and Schiller, H.: The MERIS Case 2 water algorithm, Int. J. Remote Sens., 28, 517–535, doi:10.1080/01431160600821127, 2007. 2160, 2167, 2168, 2177

Doerffer, R. and Schiller, H.: MERIS Lake Water Algorithm for BEAM, Algorithm Theoretical Basis Document (ATBD) Version 1.0, GKSS GmbH, Geesthacht, 2008. 2160, 2167

Doerffer, R., Sorensen, K., and Aiken, J.: MERIS potential for coastal zone applications, Int. J. Remote Sens., 20, 1809–1818, doi:10.1080/014311699212498, 1999. 2160

Elmgren, R.: Understanding human impact on the Baltic ecosystem: changing views in recent decades, Ambio, 30, 222–231, doi:10.1579/0044-7447-30.4.222, 2001. 2162

European Space Agency: MERIS Product Handbook, available at: http://envisat.esa.int/handbooks/meris/, 2011. 2160

Franzén, F., Kinell, G., Walve, J., Elmgren, R., and Söderqvist, T.: Participatory social-ecological modeling in eutrophication management: the case of Himmerfjärden, Sweden, Ecol. Soc., 16(4): 27, doi:10.5751/ES-04394-160427, 2011. 2163

González Vilas, L., Spyrakos, E., and Torres Palenzuela, J. M.: Neural network estimation of chlorophyll *a* from MERIS full resolution data for the coastal waters of Galician rias (NW Spain), Remote Sens. Environ., 115, 524–535, doi:10.1016/j.rse.2010.09.021, 2011. 2178

Gregg, W. W. and Conkright, M. E.: Global seasonal climatologies of ocean chlorophyll: blending in situ and satellite data for the coastal zone color scanner era, J. Geophys. Res.-Oceans, 106, 2499–2515 2001. 2160

Heim, B., Overduin, P., Schirrmeister, L., and Doerffer, R.: OCOC – from Ocean Colour to Organic Carbon, Proc. of the 2nd MERIS/(A)ATSR User Workshop, Frascati, Italy, 22–26 September 2008 (ESA SP-666, November 2008), 2008. 2178

IOCCG: Report 10. Atmospheric correction for remotely-sensed ocean-colour products, IOCCG, International Ocean-Colour Coordinating Group, Canada, CA, 2010. 2159, 2160

Jeffrey, S. W. and Humphrey, G. F.: New spectrophotometric equations for determining chlorophylls a, b, c_1 and c_2 in higher plants, algae and natural phytoplankton, Biochem. Physiol. P., 167, 191–194, 1975. 2163

Kirk, J. T. O.: Light and Photosynthesis in Aquatic Environments, Cambridge University Press, 2nd edn., 1994. 2163

Koponen, S., Ruiz-Verdu, A., Heege, T., Heblinski, J., Sorensen, K., Kallio, K., Pyhälahti, T., Doerffer, R., Brockmann, C., and Peters, M.: Development of MERIS lake water algorithms, Validation report, ESRIN Contract No. 20436/06/I-LG, 2008. 2168

Kratzer, S.: Bio-optical Studies of Coastal Waters, Ph. D. thesis, University of Wales, Bangor. School of Ocean Sciences, Menai Bridge, Anglesey, LL59 5EY, UK, 2000. 2163, 2164

Kratzer, S. and Tett, P.: Using bio-optics to investigate the extent of coastal waters: a Swedish case study, Hydrobiologia, 629, 169–186, doi:10.1007/s10750-009-9769-x, 2009. 2162, 2179

Kratzer, S. and Vinterhav, C.: Improvement of MERIS level 2 products in Baltic Sea coastal areas by applying the Improved Contrast between Ocean and Land processor (ICOL) – data analysis and validation, Oceanologia, 32, 211–236, available at: http://swepub.kb.se/bib/swepub:oai:DiVA.org:su-49204?tab2=abs&language=en, 2010. 2161, 2165, 2169

Kratzer, S., Brockmann, C., and Moore, G.: Using MERIS full resolution data to monitor coastal waters – a case study from Himmerfjärden, a fjord-like bay in the northwestern Baltic Sea, Remote Sens. Environ., 112, 2284–2300, doi:10.1016/j.rse.2007.10.006, 2008. 2161, 2164, 2165, 2180

Kutser, T.: Quantitative detection of chlorophyll in cyanobacterial blooms by satellite remote sensing, Limnol. Oceanogr., 49, 2179–2189, 2004. 2178

Kutser, T., Paavel, B., Metsamaa, L., and Vahtmäe, E.: Mapping coloured dissolved organic matter concentration in coastal waters, Int. J. Remote Sens., 30, 5843–5849, 2009. 2162

Laur, H.: ENVISAT and ERS missions, available at: http://envisat.esa.int/handbooks/meris/, 2012. 2160

Leppèaranta, M. and Myrberg, K.: Physical Oceanography of the Baltic Sea, Springer Praxis Books, Springer, Berlin, Heidelberg, doi:10.1007/978-3-540-79703-6, 2009. 2162

Maslowski, W. and Walczowski, W.: Circulation of the Baltic Sea and its connection to the Pan-Arctic region – a large scale and high-resolution modeling approach, Boreal Env. Res., 7, 319–325, 2002. 2168

MERIS_ESL: MERIS smile effect characterisation and correction, Tech. rep., ESA, technical note, 2008. 2167

Mobley, C. D.: Light and Water, Radiative Transfer in Natural Waters, vol. 592, Academic Press, 1994. 2159

Moore, G., Icely, J., and Kratzer, S.: Field Inter-comparison and validation of in-water radiometer and sun photometers for MERIS validation, Proceedings of the ESA Living Planet Symposium, Special Publication SP-686, 2010. 2165

Morel, A. and Prieur, L.: Analysis of variations in ocean color, Limnol. Oceanogr., 22, 709–722, doi:10.4319/lo.1977.22.4.0709, 1977. 2159

Nelson, N. B. and Siegel, D. A.: The global distribution and dynamics of chromophoric dissolved organic matter, Ann. Rev. Mar. Sci., 5, 447–476, doi:10.1146/annurev-marine-120710-100751, 2013. 2159

Ohde, T., Siegel, H., and Gerth, M.: Validation of MERIS Level-2 products in the Baltic Sea, the Namibian coastal area and the Atlantic Ocean, Int. J. Remote Sens., 28, 609–624, doi:10.1080/01431160600972961, 2007. 2161

Park, Y., Van Mol, B., and Ruddick, K.: Validation of MERIS water products for Belgian coastal waters, in: Proceedings of MERIS and AATSR calibration and geographical validation validation workshop, 1, ESA, Frascati, 2004. 2176

Parsons, T. R., Maita, Y., and Lalli, C. M.: A manual of chemical and biological methods for seawater analysis, XIV, Pergamon Press, Oxford, UK, 1984. 2163

Philipson, P., Kratzer, S., Krusper, A., and Strömbeck, N.,: Final report – Satellite products development for water quality monitoring in the great lakes and Himmerfjärden, 2009. 2161

Prieur, L. and Sathyendranath, S.: An optical classification of coastal and oceanic waters based on the specific spectral absorption curves of phytoplankton pigments, dissolved organic matter, and other particulate materials, Limnol. Oceanogr., 26, 671–689, 1981. 2159

Reinart, A. and Kutser, T.: Comparison of different satellite sensors in detecting cyanobacterial bloom events in the Baltic Sea, Remote Sens. Environ., 102, 74–85, doi:10.1016/j.rse.2006.02.013, 2006. 2176

Roesler, C. S. and Boss, E.: In situ measurement of the Inherent Optical Properties (IOPs) and potential for harmful algal bloom detection and coastal ecosystem observations, in: Real-time Coastal Observing Systems for Marine Ecosystem Dynamics and Harmful Algal Blooms. Theory, instrumentation and modelling, edited by: Babin, M., Roesler, C., and Cullen, J. J., UNESCO Publishing, Paris, 2008. 2178

Santer, R. and Zagolski, F.: ICOL ATBD, Tech. Rep. version 0.1, Université du Littoral, Wimereux, France, 2007. 2161

Santer, R. and Zagolski, F.: ICOL-Improve contrast between ocean & land, ATBD-The MERIS Level 1-C, Tech. Rep. version 1.1, Université du Littoral, Wimereux, France, 2009. 2161, 2166

Schroeder, T., Behnert, I., Schaale, M., Fischer, J., and Doerffer, R.: Atmospheric correction algorithm for MERIS above case-2 waters, Int. J. Remote Sens., 28, 1469–1486, doi:10.1080/01431160600962574, 2007a. 2160, 2167

Schroeder, T., Schaale, M., and Fischer, J.: Retrieval of atmospheric and oceanic properties from MERIS measurements: a new Case-2 water processor for BEAM, Int. J. Remote Sens., 28, 5627–5632, doi:10.1080/01431160701601774, 2007b. 2160, 2167, 2168

Schwarz, J., Kowalczuk, P., Kaczmarek, S., Cota, G., Mitchell, B., Kahru, M., Chavez, F., Cunningham, A., McKee, D., Gege, P., Kishino, M., Phinney, D., and Raine, R.: Two models for absorption by coloured dissolved organic matter (CDOM), Oceanologia, 44, 209–241, 2002. 2176

Sørensen, K., Grung, M., and Röttgers, R.: An intercomparison of in vitro chlorophyll *a* determinations for MERIS level 2 data validation, Int. J. Remote Sens., 28, 537–554, doi:10.1080/01431160600815533, 2007. 2164, 2180

Stramski, D., Boss, E., Bogucki, D., and Voss, K. J.: The role of seawater constituents in light backscattering in the ocean, Prog. Oceanogr., 61, 27–56, doi:10.1016/j.pocean.2004.07.001, 2004. 2178

Strickland, J. and Parsons, T.: A Practical Handbook of Seawater Analysis, Fisheries Research Board of Canada Series, Fisheries Research Board of Canada, 1972. 2163

Title Page
Abstract | Introduction
Conclusions | References
Tables | Figures
I◀ | ▶I
◀ | ▶
Back | Close
Full Screen / Esc
Printer-friendly Version
Interactive Discussion

Vaičiūtė, D., Bresciani, M., and Bučas, M.: Validation of MERIS bio-optical products with in situ data in the turbid Lithuanian Baltic Sea coastal waters, J. Appl. Remote Sens., 6, 063568–1, 2012. 2161, 2179

Zhang, T.: Retrieval of oceanic constituents with artificial neural network based on radiative transfer simulation techniques, Ph. D. thesis, Freie Universität, Berlin, 2003. 2168

Zibordi, G., Ruddick, K., Ansko, I., Moore, G., Kratzer, S., Icely, J., and Reinart, A.: In situ determination of the remote sensing reflectance: an inter-comparison, Ocean Sci., 8, 567–586, doi:10.5194/os-8-567-2012, 2012. 2164, 2165, 2173

Title Page
Abstract | Introduction
Conclusions | References
Tables | Figures
◀ | ▶
◀ | ▶
Back | Close
Full Screen / Esc
Printer-friendly Version
Interactive Discussion

Table 1. Level 1b processing schemes applied.

Acronym	Description
SC	Smile correction
EQ	Equalization of coherent noise
SCEQ_L1N	Dataset with both SCEQ corrections where ICOL has been applied
SCEQ_X	Dataset with both SCEQ corrections where ICOL has not been applied

Table 2. Matchups timetable. Note: Cast ID refers to the site, number of transect, and sampling id.

		Time [UTM]			MERIS matchup window			
cast ID	date	in situ	overpass	cloudy	< 30 min	≤ 1 h	≤ 2 h	≫ 2 h
BIII_1a	9 Jul 2008	09:14:00	09:25:41		*			
H3_2b		09:45:00	09:37:05		*			
H4_2c		10:45:00	09:37:05			*		
H5_3a	18 Jul 2008	08:03:00	09:42:46				*	
H4_3b		09:00:00	09:42:46			*		
H3_3c		09:45:00	09:42:46		*			
H2_3d		10:45:00	09:42:46			*		
BY31_4a	24 Jul 2008	08:50:00	09:54:08			*		
BIII_4b		09:55:00	09:54:08		*			
BII_4c		10:45:00	09:54:08			*		
BI_4d		11:30:00	09:54:08				*	
CI_5a	25 Jul 2008	08:30:00	09:22:50			*		
CII_5b		09:15:00	09:22:50		*			
CIII_5c		10:10:00	09:22:50			*		
H4_6a	28 Jul 2008	09:45:00	09:28:32		*			
H3_6b		10:35:00	09:28:32			*		
H2_6c		11:20:00	09:28:32				*	
H2_7a	30 Jul 2008	08:34:00	10:05:28				*	
CIII_8a	31 Jul 2008	08:30:00	09:33:33			*		
CII_8b		10:45:00	09:33:33				*	
CI_8c		08:30:00	09:33:33			*		

Title Page
Abstract | Introduction
Conclusions | References
Tables | Figures
◀| |▶
◀ ▶
Back | Close
Full Screen / Esc
Printer-friendly Version
Interactive Discussion

Table 2. Continued.

		Time [UTM]			MERIS matchup window			
cast ID	date	in situ	overpass	cloudy	< 30 min	≤ 1 h	≤ 2 h	≫ 2 h
B1_1a	5 May 2010	08:44:00	09:24:41	*		*		
H2_1b		11:30:00	09:24:41				*	
BI_2a	11 May 2010	08:30:00	09:36:08			*		
BII_2b		09:45:00	09:36:08		*			
BIII_2c		11:05:00	09:36:08				*	
B1_3a	18 May 2010	07:57:00	09:16:04	*			*	
BI_3b		10:12:00	09:16:04			*		
BII_3c		12:27:00	09:16:04					*
BI_4a	20 May 2010	08:01:00	09:53:22	*			*	
BII_4b		09:25:00	09:53:22	*	*			
BIII_4c		10:32:00	09:53:22	*		*		
BY31_4d		11:35:00	09:53:22				*	
B1_5a	24 May 2010	08:15:00	09:27:34				*	
H2_5b		09:25:00	09:27:34		*			
H3_5c		10:46:00	09:27:34			*		
H4__6a	20 Aug 2010	08:20:00	10:02:02	*			*	
H2_6b		10:10:00	10:02:02		*			
B1_6c		11:30:00	10:02:02	*			*	

Table 3. Ranges of optical water constituent concentrations that defines the training range of level 2 processors used here.

	FUB		MEGS		C2R		BOREAL	
water constituent	Min	Max	Min	Max	Min	Max	Min	Max
[CHL, mg m^{-3}]	0.05	50	0.02	43	0.003	50	0.5	50
[SPM, g m^{-3}]	0.05	50	0.01	51	0.03	50	0.1	20
$aCDOM_{440}$, m^{-1}	0.005	1.0	0.005	5	0.002	2	0.25	10

Title Page
Abstract | Introduction
Conclusions | References
Tables | Figures
◂◂ | ▸▸
◂ | ▸
Back | Close
Full Screen / Esc
Printer-friendly Version
Interactive Discussion

Table 4. In situ water constituent concentrations.

water constituent	in situ mean [median] ± stdev	*n*	Min	Max
[CHL, $\mathrm{mg\,m^{-3}}$]	3.98[2.68] ± 3.60	38	0.92	22.53
[SPM, $\mathrm{g\,m^{-3}}$]	1.46[1.34] ± 0.69	38	0.30	3.25
$\mathrm{aCDOM_{440}}$, $\mathrm{m^{-1}}$	0.45[0.40] ± 0.11	17	0.36	0.82

Table 5. Quality flags used for pixel exclusion criteria within a 3 × 3 pixel-matrix.

L2 processor	geophysical product	Raised flags
MEGS	algal_2, yellow_subs, total_susp	land, suspect, pcd_1_13, pcd_17
	radiometry	land, suspect, pcd_1_13
FUB	algal_2	LEVEL1b_masked, CHL_IN, CHL_OUT
	yellow_subs	LEVEL1b_masked, YEL_IN, YEL_OUT
	total_susp	LEVEL1b_masked, TSM_IN, TSM_OUT
	radiometry	LEVEL1b_masked, l1_flags > 2, ATM_OUT
C2R	chl_conc, a_ys_443, tsm	case2_flags, agc_flags, l1_flags > 2,
	radiometry	agc_flags, l1_flags > 2
BOREAL	chl_conc, a_ys_443, tsm	case2_flags, agc_flags, l1_flags > 2,
	radiometry	agc_flags, l1_flags > 2

Table 6. Summary of error analysis for $\rho(\lambda)$ against sea-truthing data using common macro pixels ($n = 16$).

Processor	λ	MNB [%]	RMS_{RD} [%]	r
FUB	413	−23.38	35.91	0.11
	443	−26.86	26.66	0.35
	490	−22.18	18.47	0.66
	510	−26.33	13.82	0.77
	560	−29.28	11.76	0.84
	620	−29.70	16.59	0.75
	665	−32.58	16.19	0.77
MEGS	413	−35.23	65.87	0.33
	443	−18.91	41.47	0.47
	490	−12.67	21.52	0.77
	510	−15.71	17.25	0.82
	560	−12.84	13.39	0.91
	620	−6.65	17.72	0.84
	665	−10.04	19.47	0.78
C2R	413	28.10	81.60	0.52
	443	20.38	61.70	0.56
	490	17.64	43.92	0.69
	510	−1.12	28.28	0.78
	560	−8.01	17.99	0.87
	620	4.55	20.46	0.81
	665	−12.26	19.58	0.77

Table 7. Summary of error analysis for [CHL] compared to sea-truthing using common macro pixels by each pair of processors.

Pair	Processor	*n*	MNB [%]	$\mathrm{RMS_{RD}}$ [%]
FUB_MEGS	FUB	16	**26.53**	**54.46**
	MEGS		62.23	86.93
C2R_FUB	C2R	21	73.59	119.65
	FUB		**17.77**	**52.28**
C2R_MEGS	C2R	21	82.83	109.91
	MEGS		56.76	77.38
BOREAL_MEGS	BOREAL	11	241.39	169.70
	MEGS		96.45	81.51
BOREAL_FUB	BOREAL	11	266.79	211.02
	FUB		45.79	53.48
BOREAL_C2R	BOREAL	14	239.22	193.90
	C2R		110.14	104.86

Title Page
Abstract
Introduction
Conclusions
References
Tables
Figures
◀|
|▶
◀
▶
Back
Close
Full Screen / Esc
Printer-friendly Version
Interactive Discussion

Table 8. Summary of error analysis for [SPM] compared to sea-truthing data using common macro pixels by each pair of processors.

Pair	Processor	n	MNB [%]	$\mathrm{RMS}_{\mathrm{RD}}$ [%]
FUB_MEGS	FUB	16	**−27.46**	**43.66**
	MEGS		**7.85**	**39.87**
C2R_FUB	C2R	21	**5.50**	50.56
	FUB		−37.05	**42.46**
C2R_MEGS	C2R	21	**25.21**	**47.81**
	MEGS		**16.16**	**42.42**
BOREAL_MEGS	BOREAL	11	76.95	61.82
	MEGS		35.70	33.53
BOREAL_FUB	BOREAL	11	47.52	78.52
	FUB		−25.90	42.64
BOREAL_C2R	BOREAL	14	54.87	73.11
	C2R		32.54	47.71

Table 9. Summary of error analysis for aCDOM compared to sea-truthing data using common macro pixels by each pair of processors.

Pair	Processor	n	MNB [%]	$\mathrm{RMS}_{\mathrm{RD}}$ [%]
FUB_MEGS	FUB	5	−68.35	7.04
	MEGS		−89.89	2.56
C2R_FUB	C2R	7	−88.71	2.68
	FUB		−68.64	5.16
C2R_MEGS	C2R	6	−89.11	2.38
	MEGS		−90.08	2.34

Table 10. Summary of error analysis for [CHL] and [SPM] by year compared to sea-truthing data using individual best macro pixels.

Processor	water product	year	n	MNB [%]	$\mathrm{RMS}_{\mathrm{RD}}$ [%]
FUB	[CHL]	2008	16	15.5	60.9
		2010	10	24.1	108.2
		both	26	18.8	80.4
	[SPM]	2008	9	−47.0	55.8
		2010	10	−40.2	50.4
		both	19	−43.4	51.6
MEGS	[CHL]	2008	15	56.6	70.0
		2010	6	55.8	102.0
		both	21	56.4	77.6
	[SPM]	2008	9	22.5	51.7
		2010	6	−0.9	42.3
		both	15	13.1	48.0
C2R	[CHL]	2008	19	58.9	95.5
		2010	8	88.9	134.3
		both	27	67.7	106.6
	[SPM]	2008	19	19.6	55.4
		2010	8	3.8	46.6
		both	27	14.9	52.6

Table 11. Summary of error analysis for [CHL] and [SPM] by year compared to a subset of sea-truthing data using individual best macro pixels.

Processor	water product	year	n	MNB [%]	$\mathrm{RMS}_{\mathrm{RD}}$ [%]
FUB	[CHL]	2008	9	−28.5	37.1
		2010	10	24.1	108.2
		both	19	−0.8	84.8
	[SPM]	2008	9	−47.0	55.8
		2010	10	−40.2	50.4
		both	19	−43.4	51.6
MEGS	[CHL]	2008	9	23.1	36.9
		2010	6	55.8	102.0
		both	15	36.2	69.0
	[SPM]	2008	9	22.5	51.7
		2010	6	−0.9	42.3
		both	15	13.1	48.0

Table 12. Acronym list.

Abbrevation	Description	Unit/Version	Category
CHL, Chl *a*	phytoplankton pigments with Chlorophyll *a* as proxy	mg m^{-3}	Water constituent
SPM	Suspended Particulate Matter	g m^{-3}	Water constituent
CDOM, aCDOM	Coloured Dissolve Organic Matter and its absorption measured at 440 nm	m^{-1}	Water constituent
YEL-BPA	Yellow substances and Bleached Particle Absorption	m^{-1}	Water constituent
AMORGOS	Accurate MERIS Ortho-Rectified Geo-location Operational Software		Software
BEAM	Earth Observation Toolbox and Development Platform	v.4.10.3	Software
ODESA	Optical data processor of the European Space Agency		Software
TACCS	Tethered attenuation coefficient chain-sensor		Field radiometry instruments
MERIS	MEdium Resolution Imaging Spectrometer		Satellites and Sensors
ENVISAT	ENVIronment SATellite		Satellites and Sensors
MEGS	MERIS ground segment development platform	v.8.1	Level-2 processors
FUB	Freie Universität Berlin Water processor	v.1.2.10	Level-2 processors
C2R	Case 2 Regional	v.1.5.3	Level-2 processors
BOREAL	Lakes Boreal processor	v.1.5.3	Level-2 processors
ICOL	Improved Contrast between Ocean and Land	v.2.9.1	Level 1B data processing
EQ	Equalization of Coherent Noise		Level 1B data processing
SC	Smile Correction		Level 1B data processing
IOP	Inherent Optical Properties		Optics and radiometry
VIS	visible light of the electromagnetic spectrum [380–750 nm]	nm	Optics and radiometry
NIR	Near Infrared	nm	Optics and radiometry
TOA	Top of Atmosphere		Geolocation
MNB	Mean Normalized Bias		Statistics
RMS_{RD}	Root Mean Squared of the relative differences		Statistics

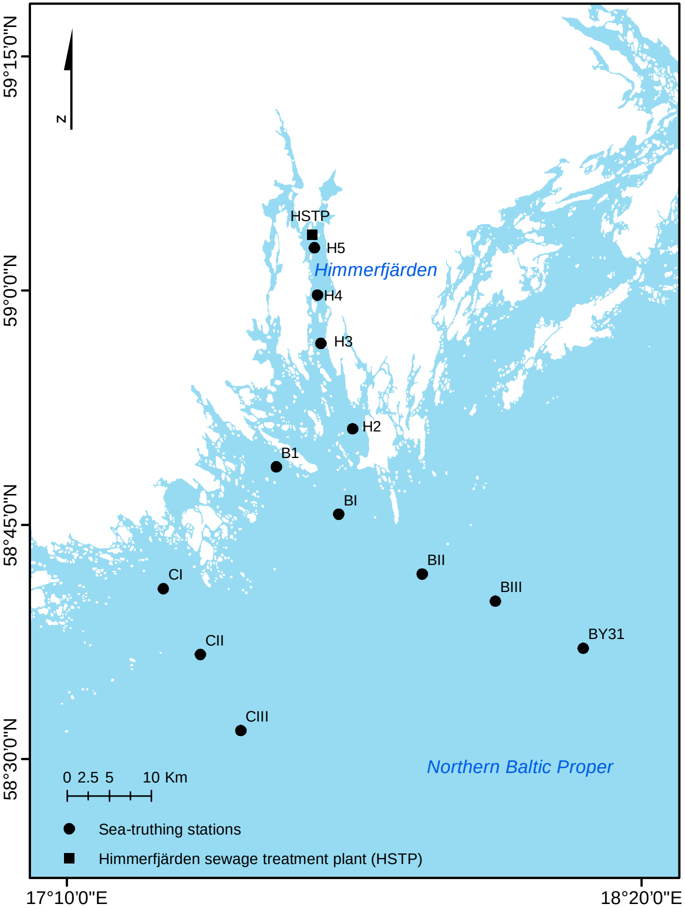

Fig. 1. Himmerfjärden is the region of interest, where sea-truthing campaigns were performed in 2008 and 2010. See Table 2 for campaign dates and time of the satellite overpasses.

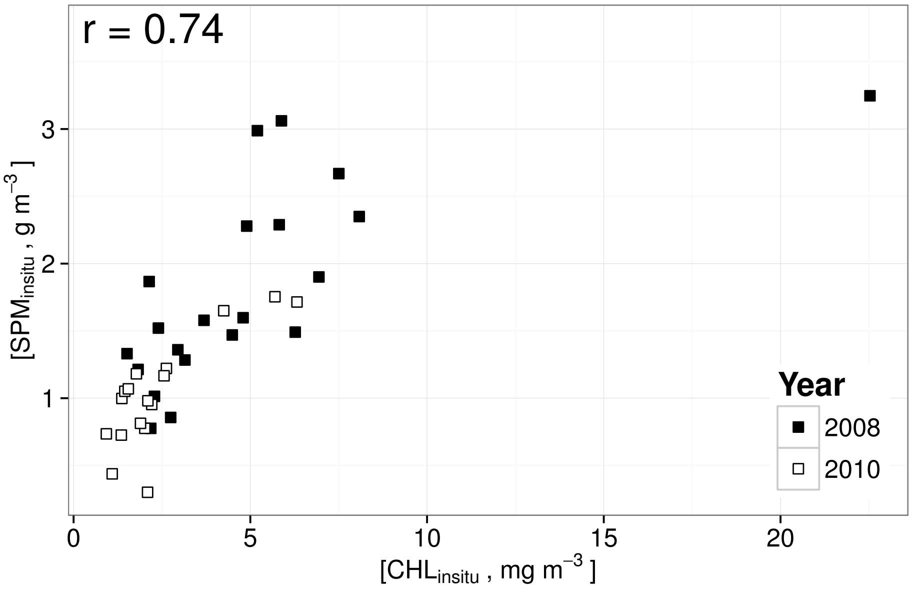

Fig. 2. Correlation between [SPM] and [CHL]. The correlation coefficient, r, was calculated for both years.

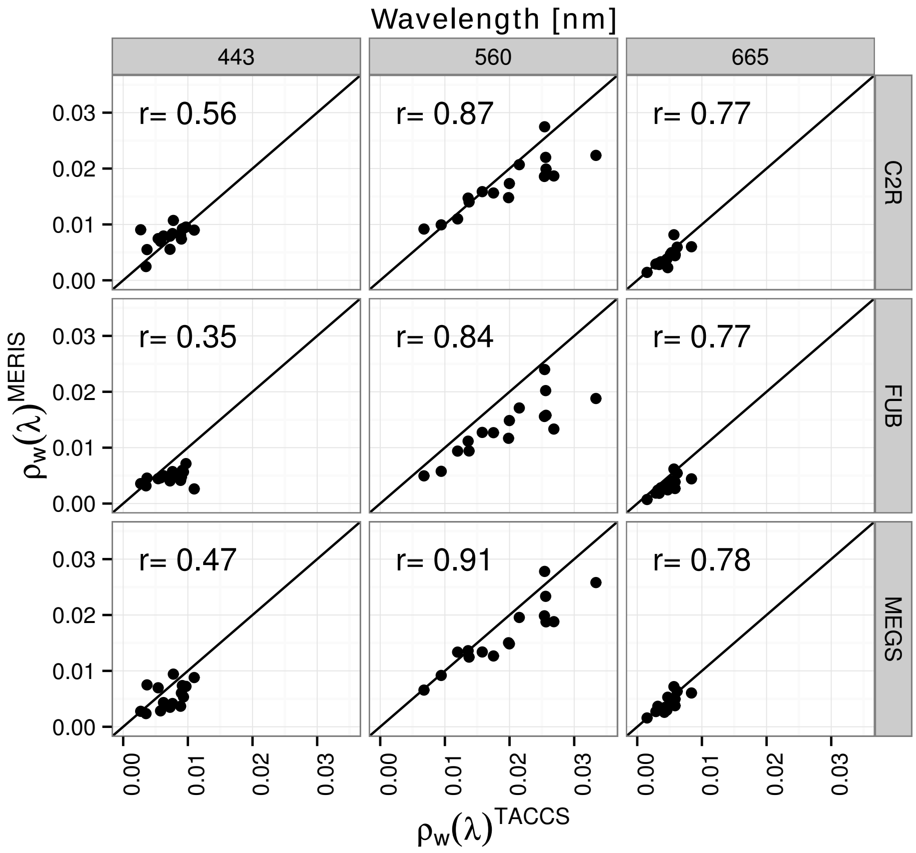

Fig. 3. Correlation between MERIS and TACCS $\rho_w(\lambda)$ for each processor using common macro pixels. The solid black line represents the 1 : 1 line. The correlation coefficient is given by r. The figure columns represent selected wavelengths: blue (443 nm), green (560 nm) and red (665). The C2R and BOREAL had the same results, so only the C2R is presented here.

Title Page
Abstract
Introduction
Conclusions
References
Tables
Figures
◀▎
▶▎
◀
▶
Back
Close
Full Screen / Esc
Printer-friendly Version
Interactive Discussion

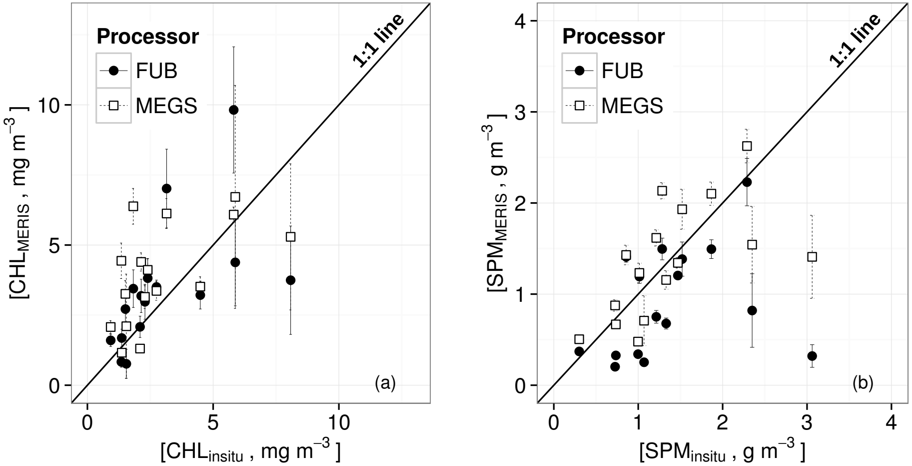

Fig. 4. Correlation for the pairwise [CHL] and [SPM] comparison between FUB vs. MEGS **(a, b)** compared to sea-truthing measurements. Data corresponds to common macro pixels. The error bars are the standard deviation of the macro pixel. The solid black line represents the 1 : 1 line.

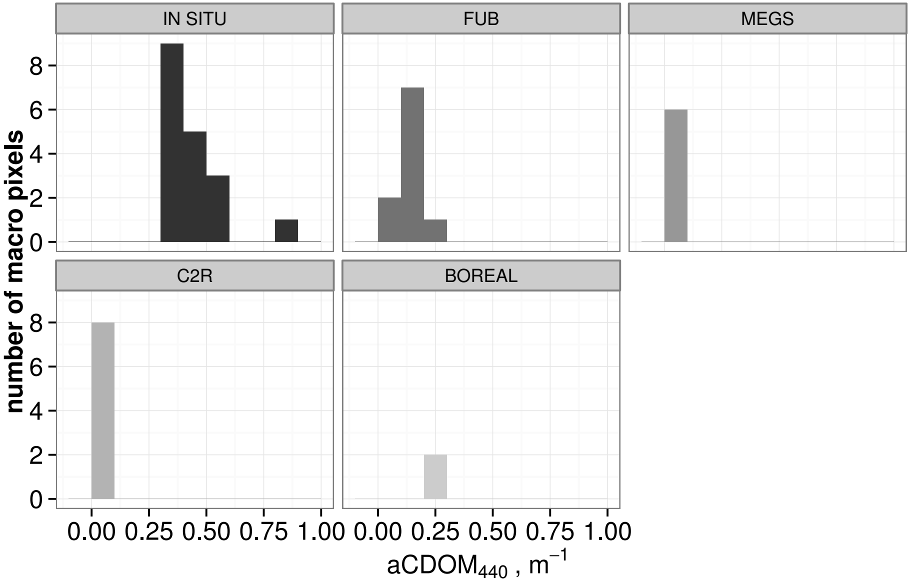

Fig. 5. Histogram showing the distribution of macro pixel CDOM absorption [m^{-1}] for each level 2 processors.

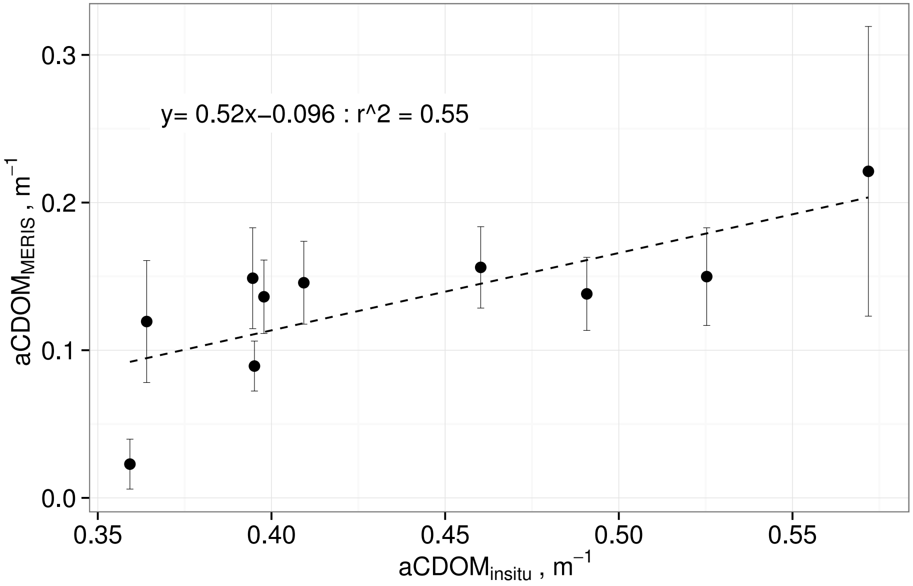

Fig. 6. Regression of aCDOM derived from FUB compared to sea-truthing data.